

Numerical Study on the Acoustic Field of a Deviated Borehole with 2.5D Method

L. Liu¹, W. J. Lin¹, H. L. Zhang¹

¹State Key Laboratory of Acoustics, Institute of Acoustics, Chinese Academy of Sciences, Beijing, China

Abstract

Acoustic well logging is important in oil exploration and development industry. Its simplified theoretical model is a waveguide structure as a cylindrical borehole filled with fluid penetrating a solid formation [Figure 1]. Nevertheless, unlike the traditional waveguide structure, the solid formation extends to infinity, which complicates the problem. Recently, offshore development adopts high angle wells to reduce drilling cost and these offshore reservoir formations often exhibit strong anisotropy [1]. For such a deviated borehole model, numerical method is needed to analyze the wave propagation.

The PDE interface of COMSOL Multiphysics® software was used to implement the 2.5D method to investigate the wave propagation in a deviated borehole penetrating a transversely isotropic formation. The variables in the model were the displacement potential in the fluid area and the displacements in the solid area respectively [2]. Besides, a convolutional perfectly matched layer [3, 4] was implemented, also using the PDE interface, to eliminate the reflections from the artificial truncation boundary, which played a good performance.

The computations were conducted in the frequency-wave number domain, so the distribution of modes could be found clearly in the direct computational results [Figure 2] and the phase velocities of the modes could be obtained easily and accurately. Waveforms in time domain [Figure 3] could also be obtained by Fourier and inverse-Fourier transform of the frequency-wave number domain results. For a dipole source, we calculated the flexural modes for different deviation angles and different dipole orientations [Figure 4]. The results show that for a deviated borehole, the flexural mode split into fast flexural mode and slow flexural mode, the velocities of which were about the SH and quasi-SV phase velocities of the formation respectively, at low frequencies [5]. Both the hard and soft formation conditions were calculated. The value of error was also presented, which show a high accuracy.

To sum up, in this paper, the 2.5D frequency-wave number domain method was used to investigate the wave propagation in a deviated borehole penetrating a transversely isotropic formation by means of the PDE interface of COMSOL Multiphysics® software. A convolutional perfectly matched layer was implemented to absorb the reflections and simulate an infinite solid area. The flexural mode in a deviated borehole was analyzed. The method used here could be extended to other more complicated models with simple modification.

Reference

1 Chi, Shihong, and Xiaoming Tang. Stoneley-wave speed modeling in general anisotropic formations. *Geophysics* 71.4 (2006): F67-F77.

2 Zhang, Hailan, Weijun Lin, and Xiuming Wang. Numerical Studies on the Acoustic Field Generated by a Dipole Source in Noncircular Pipes. *REVIEW OF PROGRESS IN QUANTITATIVE NONDESTRUCTIVE EVALUATION: Volume 30A; Volume 30B* 1335.1 (2011): 1424-1431.

3 Li, YiFeng, and Olivier Bou Matar. Convolutional perfectly matched layer for elastic second-order wave equation. *The Journal of the Acoustical Society of America* 127.3 (2010): 1318-1327.

4 Komatitsch, Dimitri, and Roland Martin. An unsplit convolutional perfectly matched layer improved at grazing incidence for the seismic wave equation. *Geophysics* 72.5 (2007): SM155-SM167.

5 He, Xiao, Hengshan Hu, and Wei Guan. Fast and slow flexural waves in a deviated borehole in homogeneous and layered anisotropic formations. *Geophysical Journal International* 181.1 (2010): 417-426.

Figures used in the abstract

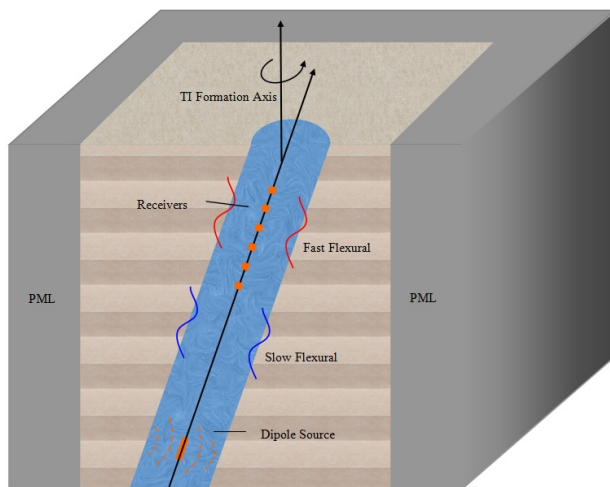


Figure 1: Model of a deviated borehole penetrating a transversely isotropic formation.

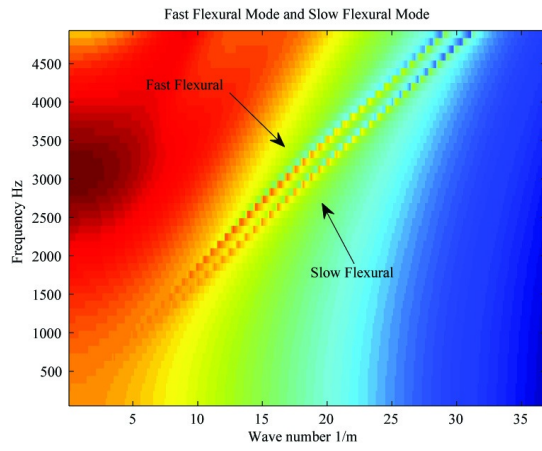


Figure 2: Flexural mode in the frequency-wave number domain.

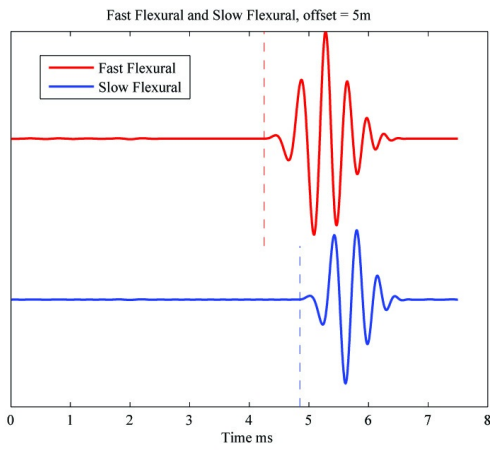


Figure 3: Waveform for different dipole source orientation.

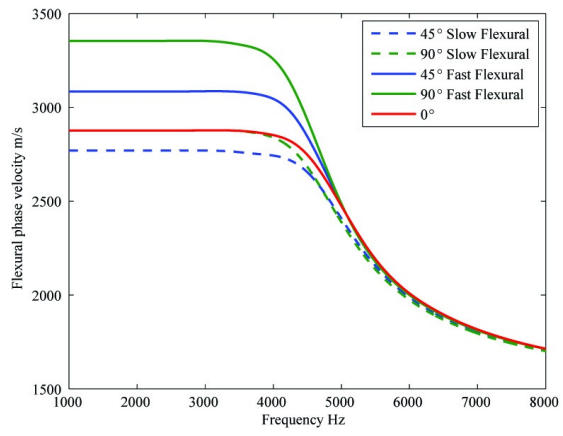


Figure 4: Flexural phase velocities.